GA–A24352

ELECTRON TEMPERATURE FLUCTUATIONS AND CROSS-FIELD HEAT TRANSPORT IN THE EDGE OF DIII–D

by
D.L. RUDAKOV, J.A. BOEDO, R.A. MOYER, S. KRASENINNIKOV,
M.A. MAHDAVI, G.R. McKEE, G.D. PORTER, P.C. STANGEBY,
J.G. WATKINS, W.P. WEST, and D.G. WHYTE

JULY 2003

DISCLAIMER

GA–A24352

ELECTRON TEMPERATURE FLUCTUATIONS AND CROSS-FIELD HEAT TRANSPORT IN THE EDGE OF DIII–D

by

D.L. RUDAKOV,* J.A. BOEDO,* R.A. MOYER,* S. KRASENINNIKOV,*
M.A. MAHDAVI, G.R. McKEE,† G.D. PORTER,‡ P.C. STANGEBY,$^{\Delta}$
J.G. WATKINS,# W.P. WEST, and D.G. WHYTE†

This is a preprint of a paper to be presented at the 30th European Physical Society Conference on Controlled Fusion and Plasma Physics, St Petersburg, Russia, July 7–11, 2003 and to be published in the *Proceedings.*

*University of California, San Diego, California.
†University of Wisconsin, Madison, Wisconsin.
‡Lawrence Livermore National Laboratory, Livermore, California.
$^{\Delta}$University of Toronto, Toronto, Canada.
#Sandia National Laboratories, Albuquerque, New Mexico.

Work supported by
the U.S. Department of Energy
under Contract Nos. DE-FG03-95ER54294,
DE-FG02-89ER53297, DE-AC03-99ER54463, W-7405-ENG-48,
and DE-AC04-94AL85000

GENERAL ATOMICS PROJECT 30033
JULY 2003

Electron Temperature Fluctuations and Cross-Field Heat Transport in the Edge of DIII-D

D.L. Rudakov,[1] J.A. Boedo,[1] R.A. Moyer,[1] S. Krasheninnikov,[1] M.A. Mahdavi,[2] G.R. McKee,[3] G.D. Porter,[4] P.C. Stangeby,[5] J.G. Watkins,[6] W.P. West,[2] D.G. Whyte[3]

[1]University of California, San Diego, La Jolla, California 92093-0417, USA
[2]General Atomics, San Diego, California 92186-5608, USA
[3]University of Wisconsin, Madison, Wisconsin 53706, USA
[4]Lawrence Livermore National Laborabory, Livermore, California 94551, USA
[5]University of Toronto Institute for Aerospace Studies, Toronto, M3H 5T6, Canada
[6]Sandia National Laboratories, Alberqueue, New Hampshire 87185-1129, USA

1. Introduction

The fluctuating $E \times B$ velocity due to electrostatic turbulence is widely accepted as a major contributor to the anomalous cross-field transport of particles and heat in the tokamak edge and scrape-off layer (SOL) plasmas (e.g. [1,2] and references therein). This has been confirmed by direct measurements of the turbulent $E \times B$ transport in a number of experiments [2]. Correlated fluctuations of the plasma radial velocity v_r, density n, and temperature T_e result in time-average fluxes of particles and heat given by (for electrons) [3]:

$$\Gamma_r^{ES} = \langle n \tilde{v}_r \rangle = \frac{1}{B_\varphi} \langle \tilde{n} \tilde{E}_\theta \rangle \tag{1}$$

$$Q_r^{ES} = \langle n\, T_e\, \tilde{v}_r \rangle \approx \frac{3}{2}\, kT_e \Gamma_r^{ES} + \frac{3\, n_e}{2\, B_\varphi} \langle k\tilde{T}_e \tilde{E}_\theta \rangle = Q_{conv} + Q_{cond} \quad . \tag{2}$$

The first term in Eq. (2) is referred to as convective and the second term as conductive heat flux. Experimental determination of fluxes given by Eqs. (1) and (2) requires simultaneous measurements of the density, temperature and poloidal electric field fluctuations with high spatial and temporal resolution. Langmuir probes provide most readily available (if not the only) tool for such measurements. However, fast measurements of electron temperature using probes are non-trivial and are not always performed. Thus, the contribution of the T_e fluctuations to the turbulent fluxes is usually neglected. Here we report results of the studies of T_e fluctuations and their effect on the cross-field transport in the SOL of DIII-D.

2. Experimental Technique

T_e fluctuations and fluctuation-induced transport are studied in edge and SOL plasmas in DIII-D using a reciprocating Langmuir probe array [4] equipped with a fast (100 kHz bandwidth) T_e diagnostic [5]. The probe head layout is shown in Fig. 1 (view from inside the vacuum vessel) and includes an ion saturation current (I_{si}) tip, two floating potential (V_f) tips, and two T_e tips separated by $a \approx 9.3$ mm in the poloidal direction. The head is oriented to achieve the best possible alignment of V_f and T_e tips without mutual shadowing. The probe enters the DIII-D SOL 18.8 cm below the outer mid-plane. More detailed description of the experimental arrangement can be found in Refs. [6,7].

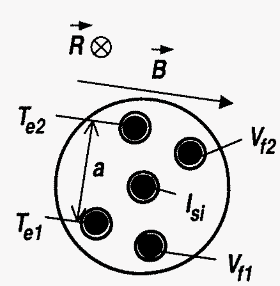

Fig. 1. Probe head layout.

3. Electron Temperature Fluctuations in DIII-D SOL

Edge T_e fluctuations in DIII-D have been studied in L and low power H-mode discharges. The fluctuations have normalized levels ranging from 0.1–0.2 at the separatrix to 0.5–0.6 in the SOL, comparable to the respective levels of the density and floating potential fluctuations. This is illustrated in Fig. 2(a) showing radial profiles (versus the distance from the separatrix, ΔR_{sep}) of the temperature and floating potential fluctuation levels in an L-mode discharge. The fluctuations are broadband with significant energy throughout the measurable range (up to 100 kHz). Sample frequency spectra of the temperature and floating potential fluctuations in L-mode are shown in Fig. 2(b). The shapes of T_e and V_f spectra are generally close, but V_f spectra fall off more rapidly with frequency.

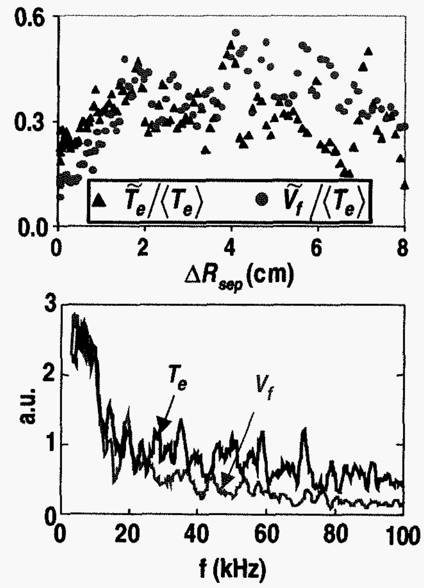

Fig. 2. Relative RMS levels of the temperature and floating potential fluctuations (a) and typical fluctuation spectra (b) in L-mode.

Since the T_e fluctuation level is considerable, those fluctuations should be properly accounted for when calculating the fluctuation-induced particle and heat fluxes from the probe data. The plasma potential is given by $V_p = V_f + C(kT_e/e)$ where $C \sim 3$ for deuterium plasmas [1], so a considerable error can be introduced if the poloidal electric field is calculated from two poloidally separated measurements of V_f rather than V_p. Still, if the density and temperature fluctuations are exactly in phase ($\alpha_{nTe} = 0$), the correction to the poloidal electric field due to the temperature fluctuation would be 90 degrees out of phase with both temperature and density and would not affect the measured fluctuation-induced fluxes [Eqs. (1–2)]. Another case when the contribution of the T_e fluctuations to E_θ can be neglected is if poloidal wave numbers (k_θ) of the T_e fluctuations are much smaller than those of V_f fluctuations. Neither condition is quite valid in DIII-D. Figure 3 shows radial profiles of the phase angle between n_e, T_e and V_f fluctuations (a) and poloidal wave numbers of T_e and V_f fluctuations (b) in L-mode. The values are averaged over the frequency range of 2–15 kHz where the fluctuations are most coherent and amplitudes are largest (most of the fluctuation-induced transport occurs in this frequency range). Though the phase angle between the density and temperature fluctuations is generally small ($\alpha_{nTe} \sim 15$ degrees), the temperature correction to E_θ may still be significant [$C \sin(\alpha_{nTe}) \approx 0.8$]. Poloidal wave numbers of the T_e fluctuations are close to those of V_f in the near SOL. In the far SOL they are smaller by a factor of 2–3, further reducing their contribution to E_θ but not canceling it completely.

4. Fluctuation-Driven Particle and Heat Fluxes in DIII-D SOL

Fluctuation-driven particle flux and both convective and conductive components of the heat flux were measured in L and H-mode discharges with and without edge localized modes (ELMs). Figure 4 presents radial profiles (within the first 2 cm outside the separatrix) of the convective, conductive, and total (note different scale) heat fluxes in three different plasma discharges: an L-mode discharge (open circles) and two H-mode discharges. One of the

H-mode discharges (solid diamonds) had comparatively long ELM-free intervals, whereas the other one (open squares) was ELMing rapidly. All data are averaged over 1 ms. In all three cases the two terms of the heat flux are comparable throughout most of the SOL except near the separatrix in L-mode where the convective component is appreciably larger than the conductive one. Conductive flux in L-mode tends to reverse direction at the separatrix, becoming radially inward. The total flux, however, remains radially outward. The net flux between the ELMs in H-mode is well below the L-mode level through most of the SOL. During ELMs (marked by the arrows in Fig. 4) local fluxes increase to or above L-mode levels. The high flux level near the separatrix in the ELM-free H-mode case is due to a coherent mode localized in that region [7]. Interestingly enough, this coherent mode drives fluxes exceeding L-mode levels (and comparable to fluxes driven by ELMs) without appreciable degradation of confinement. Coherent and quasi-coherent modes are often observed near the separatrix in H-mode discharges between ELMs, their effect on the edge gradients and ELM generation is yet to be quantified.

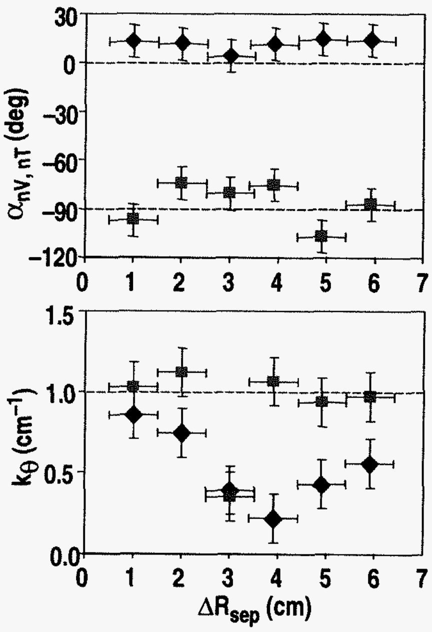

Fig. 3. Radial profiles of: (a) phase angles between n_e and V_f (squares) and n_e and T_e (diamonds) fluctuations; (b) poloidal wave numbers of V_f (squares) and T_e (diamonds) fluctuations.

The fluctuations of both electron density and temperature in DIII-D SOL have strongly non-Gaussian statistics [6–8] characterized by positive skewness (i.e. there are more positive events than negative ones) and kurtosis (i.e. there are more large events than a random distribution would have). Conditional averaging was used to characterize typical events in fluctuations and fluxes [6,7]. Spikes in the plasma density were shown to correlate with those in the poloidal electric field resulting in intermittent transport events carrying both particles and heat. The intermittence has qualitatively similar character in L-mode and high density H-mode both between and during ELMs [7]. In absolute terms, the transport rates due to intermittence during ELMs are comparable to or higher than those in L-mode [7]; between ELMs they are significantly lower. Figure 5 shows the contribution of intermittent events to the net particle and heat fluxes as a function of the relative (normalized to the mean flux) amplitude of events. Each point represents the integral fraction of the total flux carried

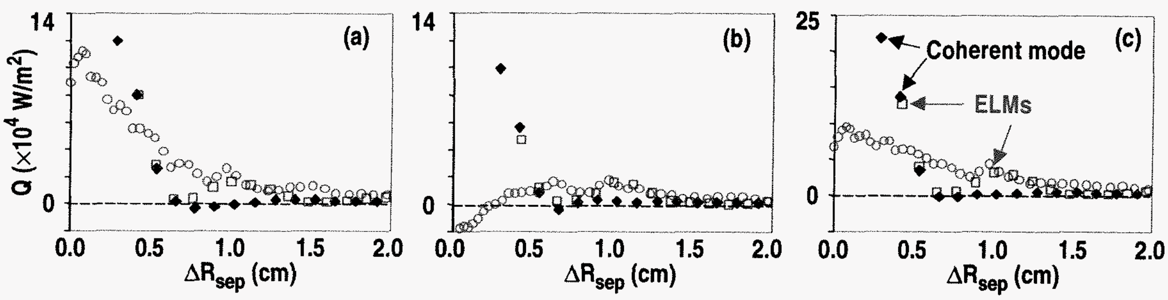

Fig. 4. Radial profiles of convective (a), conductive (b), and total (c) heat fluxes in L-mode (open circles), ELM-free H-mode (solid diamonds), and ELMing H-mode (open squares).

by all events with the relative amplitude above the corresponding x-axis value. Thus, events with amplitude above 10 times the mean flux level are responsible for about 60%–65% of the net particle and heat transport in L-mode and for about 30% of the net transport in H-mode.

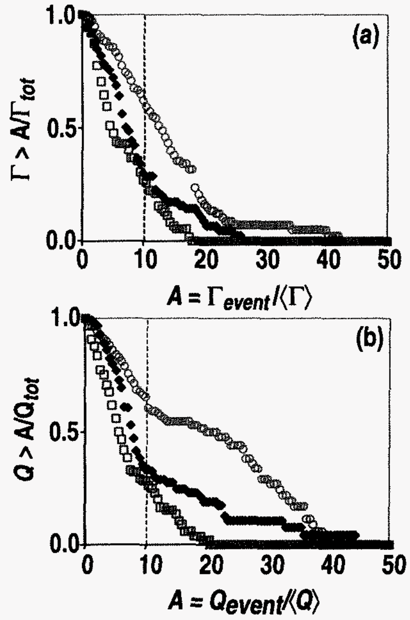

Fig. 5. Integral fraction of the total particle (a) and heat (b) flux carried by transport events with relative (normalized to the mean flux) amplitude above the x-axis value in L-mode (open circles), ELM-free H-mode (solid diamonds) and during an ELM (open squares)

5. Implications from Power Balance and Future Work

Measured values of the heat flux at the separatrix can be compared to those expected from power balance. The data of Fig. 4 have been obtained in discharges where the difference between the total input power and the total power radiated inside the separatrix was 1–1.5 MW. In L-mode, the measured heat flux at the separatrix was about 10 W/cm^2. To conduct 1.5 MW across the separatrix at this rate a toroidal band near the outer mid-plane ($R_{sep} \approx$ 230 cm) having poloidal width of about 1 meter would be sufficient. This is clearly incompatible with an assumption of poloidal symmetry of the fluctuation-induced transport. A similar result (obtained by comparison with UEDGE modeling) was previously reported for the particle transport [9]. Whether cross-field transport is indeed peaked near and below the outer mid-plane (consistent with BOUT modeling [10]) or the measured local transport rates are overestimated for some reason (e.g. [11]) is yet to be resolved. A dedicated experiment to study the poloidal dependence of fluctuations and fluctuation-induced transport is being carried out on DIII-D. The midplane reciprocating probe array has recently been modified to better conform all the tips to the same flux surface in order to improve the accuracy of the flux measurements. Hopefully, new measurements will resolve the present discrepancies.

Work supported by U.S. Department of Energy under Grants DE-FG03-95ER54294 and DE-FG02-89ER53297 and Contracts DE-AC03-99ER54463, W-7405-ENG-48, and DE-AC04-94AL85000.

[1] Stangeby, P.C., and McCracken, G.M., Nucl. Fusion **30**, 1225 (1990).
[2] Endler, M., J. Nucl. Mater. **266-269**, 84 (1999).
[3] Ross, D.W., Plasma Phys. Control. Fusion **34**, 137 (1992).
[4] Watkins, J.G., et al., Rev. Sci. Instrum. **63**, 4728 (1992).
[5] Rudakov, D.L., Boedo, J.A., Moyer, R.A., et al., Rev. Sci. Instrum. **72**, 453 (2001).
[6] Boedo, J.A., Rudakov, D.L., Moyer, R.A., et al, Phys. Plasmas **8** , 4826 (2001).
[7] Rudakov, D.L., Boedo, J.A., Moyer, R.A., et al., Plasma Phys. Control. Fusion **44**, 717 (2002).
[8] Boedo, J.A., Rudakov, D.L., Moyer, R.A., et al., Phys. Plasmas **10**, 1670 (2003)
[9] Moyer, R.A., Cuthbertson, J.W., Evans, T.E., et al., J. Nucl. Mater. **241-243**, 663 (1997).
[10] Xu, X.Q., et al., Nucl. Fusion **40**, 731 (2000); Xu, X.Q., et al., New J. Phys. **4**, 53.1 (2002).
[11] LaBombard, B., Phys. Plasmas **9**, 1300 (2002).